

- (28) J. A. Ibers, "PICK2", Northwestern University, 1966.
 (29) J. Trotter, "FOURIE", University of British Columbia, 1965.
 (30) W. R. Busing, K.O. Martin, and H. A. Levy, "ORFLS", Report ORNL-TM-305, Oak Ridge National Laboratory, Oak Ridge, Tenn., 1962.
 (31) C. K. Johnson, "ORTEP-II", Report ORNL-3794, Second Revision, Oak Ridge National Laboratory, Oak Ridge, Tenn., 1971.
 (32) B. J. Hathaway, *Struct. Bonding (Berlin)*, **14**, 49 (1973).
 (33) B. J. Hathaway and D. E. Billing, *Coord. Chem. Rev.*, **5**, 143 (1970).
 (34) L. Pauling, "The Nature of the Chemical Bond", 3rd ed, Cornell University Press, Ithaca, N.Y., 1960.
 (35) A. Camerman, *Can. J. Chem.*, **48**, 179 (1970).
 (36) This value is obtained by subtracting the radius of tetrahedral carbon (0.763 Å, Table I, ref 47) from the length of C-O bonds (1.426 Å, ref 37) for aliphatic alcohols.
 (37) L. E. Sutton, "Interatomic Distances-Supplement", *Chem. Soc., Spec. Publ.*, **No. 18** (1965).
 (38) J. Donohue, L. R. Lavine, and J. S. Rollett, *Acta Crystallogr.*, **9**, 655 (1956).
 (39) (a) E. J. Graeber and B. Morosin, *Acta Crystallogr., Sect. B*, **30**, 310 (1974); (b) A. W. Hanson, *ibid.*, **29**, 454 (1973); (c) R. D. Gilardi and I. L. Karle, *ibid.*, **28**, 1635 (1972); (d) M. Rousseaux, J. Meunier-Piret, J. Putzeys, G. Germain, and M. Van Meerssche, *ibid.*, **28**, 1720 (1972).
 (40) M. Burke-Laing and M. Laing, *Acta Crystallogr., Sect. B*, **32**, 3216 (1976).
 (41) F. Gasparri, D. Misiti, and E. Cernia, *Inorg. Chim. Acta*, **17**, L3 (1976).
 (42) N. B. Pahor, M. Calligaris, P. Delise, L. Randaccio, L. Maresca, and G. Natile, *Inorg. Chim. Acta*, **19**, 45 (1976).
 (43) R. C. Hoy and R. H. Morriss, *Acta Crystallogr.*, **22**, 476 (1967).
 (44) G. J. Palenik, *Acta Crystallogr.*, **17**, 687 (1964).
 (45) D. Betteridge and D. John, *Analyst (London)*, **98**, 377 (1973).
 (46) The visible spectra of 1-phenylazo-2-naphthol in MeOH and CHCl₃ are very similar and it is known (ref 6) that the hydrazone tautomer predominates in MeOH.
 (47) D. R. Lide, Jr., *Tetrahedron*, **17**, 125 (1962).

Metalation of Ferrocene by *n*-Butyllithium-Pentamethyldiethylenetriamine

M. Walczak,^{1a} K. Walczak,^{1a} R. Mink,^{1a} M. D. Rausch,^{1b} and Galen Stucky*^{1a}

Contribution from the Department of Chemistry and Materials Research Laboratory, University of Illinois, Urbana, Illinois 61801, and the Department of Chemistry, University of Massachusetts, Amherst, Massachusetts 01002. Received March 29, 1978

Abstract: The reaction of ferrocene with *n*-butyllithium-pentamethyldiethylenetriamine (1:3 molar ratio) results in a dilithiated ferrocene derivative which upon carbonation and subsequent hydrolysis gives the dicarboxylic acid of ferrocene. The dilithium complex exhibits dynamic behavior in benzene or toluene with both cyclopentadienyl and base exchange being observed. The crystalline product obtained from a hexane-benzene solution in the presence of pentamethyldiethylenetriamine surprisingly contains only one triamine ligand per two lithium atoms and has the empirical formula $(\eta^5\text{-C}_5\text{H}_4)_2\text{Fe}(\text{N}_3\text{C}_9\text{H}_{23})\text{-Li}_2$. The molecular structure of this complex has been determined in the solid state and has been found to be dimeric, crystallographic symmetry $\bar{1}$, with the lithium atoms in two types of environments. All three pentamethyldiethylenetriamine nitrogen atoms are coordinated to one of the unique lithium atoms while the second unsolvated lithium atom bridges between one carbon atom of a cyclopentadienyl ring from each ferrocene monomer to form the dimer. A four-center electron-deficient bridge group is consequently observed consisting of the two unsolvated lithium atoms and two carbon atoms from two different ferrocene groups. The lithium atom-iron atom distance is short, 2.667 (8) Å, and is ascribed to bonding between the ferrocene e_g molecular orbital and the unsolvated lithium atom. The compound crystallizes in the monoclinic space group, $P2_1/n$, with lattice constants of $a = 13.557$ (5) Å, $b = 10.437$ (7) Å, $c = 15.50$ (6) Å, and $\beta = 106.24$ (2)°. The calculated density is 1.170 g cm⁻³ for two dimeric units per unit cell. The crystal structure was solved by diffractometer techniques using full-matrix least-squares analysis on a total of 4331 observations. The final agreement factor was $R_2 = 0.061$ for all data.

Introduction

Electrophilic substitution reactions have often been employed in the synthesis of ferrocene derivatives.^{2a} While many common electrophilic reactions, such as chlorination or nitration, have failed to yield the desired substitution product owing to the sensitivity of the iron atom to oxidation, alkali metal reagents have been used to resolve this problem. Ferrocene is first converted to a metalated derivative, which then is reacted with the electrophile to give the desired substituted molecule. Several authors have reported 1,1'-disubstituted ferrocenes prepared in this manner.^{2,3} Rausch and Ciappenelli⁴ found that the 1,1'-dilithio intermediate can be prepared in high yield, and with almost no accompanying monolithio by-product, using *n*-butyllithium *N,N,N',N'*-tetramethylethylenediamine (TMED).

Owing to our interest in the chemistry of interactions involving main group and transition metal organometallic compounds, we decided to further examine some of the products resulting from metalation of ferrocene using *n*-butyllithium. No infrared, nuclear magnetic resonance, or X-ray structural data had been reported for any metalated ferrocenes, nor had the degree of association been determined for these compounds. We selected the dilithiated compound for initial

study. Samples of dilithioferrocene-TMED were first prepared at the University of Massachusetts.⁴⁻⁶ Efforts to obtain suitable single crystals from these samples, as well as other samples, also prepared using *n*-butyllithium-TMED at the University of Illinois, were unsuccessful. Success was finally achieved by one of the authors (M.W.) using 1,1,4,7,7-pentamethyldiethylenetriamine (PMDT) rather than TMED in the metalation reaction. We have previously found that the use of PMDT generally results in significantly more soluble products than does the base TMED. An air-sensitive, red-orange, crystalline product was isolated from the reaction of *n*-butyllithium-PMDT and ferrocene, and it was demonstrated from a carbonation study that the compound contained two lithium atoms per iron atom. However, the NMR spectrum revealed that the compound contained only one PMDT per two lithium atoms. Since the structure could not be determined from these results, an X-ray structural investigation of dilithioferrocene-pentamethyldiethylenetriamine was undertaken. The results of that study are presented below.

Our characterization of the dilithioferrocene-PMDT complex in solution by NMR also revealed some interesting molecular dynamic behavior and the results of this study are also included.

Experimental Section

Reagents and Solvents. All procedures were carried out under an inert atmosphere using either Schlenk-ware techniques or a Vacuum Atmospheres inert box. 1,1,4,7,7-Pentamethyldiethylenetriamine was purchased from Eastman Organic Chemicals. Benzene and hexane were distilled from sodium benzophenone ketyl under nitrogen and stored under an inert atmosphere.

Preparation of $[(\eta^5\text{-C}_5\text{H}_4)_2\text{Fe}(\text{N}_3\text{C}_9\text{H}_{23})\text{Li}_2]_2$. Hexane (20 mL) was added to 3.90 g (22.5 mmol) of 1,1,4,7,7-pentamethyldiethylenetriamine (PMDT). To this solution was added via syringe 15 mL of 1.5 M (22.5 mmol) *n*-butyllithium in hexane, and the resulting solution was stirred for 15 min at room temperature. A solution of ferrocene (1.39 g, 7.5 mmol) in 80 mL of warm hexane (45–50 °C) was added to the stirred *n*-butyllithium–PMDT solution, whereupon it turned orange and stirring was discontinued. Within 1 h, clusters of orange needles appeared. These were isolated by filtration, washed with hexane, and dried under vacuum. Recrystallization from hot benzene produced an overall yield of 50–60% of product in the form of red-orange plates.

Formation of 1,1'-Ferrocenedicarboxylic Acid from $[(\eta^5\text{-C}_5\text{H}_4)_2\text{Fe}(\text{N}_3\text{C}_9\text{H}_{23})\text{Li}_2]_2$. A procedure analogous to that used by Rausch and Ciappennelli⁴ was employed.

Physical Measurements. NMR samples were prepared using degassed toluene-*d*₈ as a solvent and Me₄Si as an internal standard. ¹H NMR spectra were recorded on a Varian HA-100 spectrometer. Temperatures were measured with a copper–constantan thermocouple and are considered accurate to ±2 °C.

Crystals of $[(\eta^5\text{-C}_5\text{H}_4)_2\text{Fe}(\text{N}_3\text{C}_9\text{H}_{23})\text{Li}_2]_2$ for X-ray analysis were sealed in thin-walled glass capillaries. Preliminary precession photographs showed the crystals to be monoclinic with systematic absences on *h*0*l* for *h* + *l* = 2*n* + 1 and 0*k*0 for *k* + 2*n* + 1, uniquely determining the space group as *P*2₁/*n*, a nonstandard setting for *P*2₁/*c*. An irregularly shaped block of approximate dimensions 0.3 × 0.5 × 0.6 mm was cleaved from a larger rectangular plate and used for data collection. The crystal was mounted such that the $[\bar{5}03]$ direction was coincident with the Φ axis of the diffractometer. Thirteen reflections centered on the diffractometer were used in a least-squares refinement of the lattice parameters and the following cell constants obtained: *a* = 13.557 (5) Å, *b* = 10.437 (7) Å, *c* = 15.507 (6) Å, and β = 106.24 (2)°. No experimental density was determined; the calculated density was 1.170 g/cm³ for two dimeric units per cell.

Intensity data were measured using Mo K α radiation on an automated Picker four-circle diffractometer equipped with a graphite single-crystal monochromator. Data were collected using the θ –2 θ scan technique with a scan rate of 1.0°/min. Stationary crystal–stationary counter background counts of 10 s were taken at the beginning and end of each scan. A scan width of 2.0° and a takeoff angle of 1.6° were employed for data collection. Several ω scans showed the typical full peak width at half-height to be 0.17° or less, indicating that the mosaicity was acceptably low for data collection. Three standard reflections were monitored after every 60 reflections to check crystal and counter stability.

A full form of data ($\bar{h}kl$ and *hkl*) was measured to $2\theta_{\text{max}} = 51^\circ$, giving 4331 reflections, of which 3933 were unique and 2132 classified as observed using the criterion $I_{\text{obsd}} \geq 3\sigma_c(I)$ where $\sigma_c = [T_c + 0.25(t_c/t_b)^2(B_1 + B_2)]^{1/2}$. *T*_c is the total integrated counts, *t*_c/*t*_b is the ratio of the time spent counting the peak intensity to the time spent counting the background intensities, and *B*₁ and *B*₂ are the background counts. Owing to the irregular crystal shape, no absorption correction was made ($\mu = 7.40 \text{ cm}^{-1}$). The remainder of the data collection details are the same as previously reported.⁷

The structure was solved using the heavy atom method. The coordinates of the iron atom were obtained from a Patterson map, giving an $R_1 = \Sigma(|F_o| - |F_c|)/\Sigma|F_o|$ of 0.500. Positions for all ten cyclopentadienyl ring carbon atoms, all three PMDT nitrogen atoms, and seven PMDT carbon atoms were found from the Fourier phased by the iron atom; inclusion of these atoms lowered *R*₁ to 0.314. After location of all the remaining nonhydrogen atoms, except one lithium atom, several full-matrix least-squares cycles varying both positional and isotropic thermal parameters gave *R*₁ = 0.142 at convergence. Another difference Fourier then revealed the position of the second lithium atom. Each hydrogen atom was then added using HYGEN at a calculated position 1.00 Å from the carbon atom to which it was bonded, and given that carbon atom's isotropic thermal parameter. Continued refinement of all nonhydrogen atom positions and isotropic thermal parameters after changing to a counting statistics weighting

Table I. Positional Parameters for the Nonhydrogen Atoms in Dilithioferrocene PMDT

atom	<i>x</i>	<i>y</i>	<i>z</i>
Fe	0.099 62 (6)	0.082 46 (8)	0.343 27 (5)
C(1)	−0.0208 (4)	0.1073 (5)	0.4042 (4)
C(2)	−0.0547 (4)	0.0689 (6)	0.3121 (4)
C(3)	−0.0253 (5)	0.1572 (9)	0.2548 (4)
C(4)	0.0304 (6)	0.2526 (7)	0.3078 (6)
C(5)	0.0314 (5)	0.2224 (6)	0.3962 (4)
C(6)	0.1980 (4)	−0.0524 (6)	0.4259 (4)
C(7)	0.1600 (5)	−0.0940 (6)	0.3323 (4)
C(8)	0.1859 (6)	−0.0049 (9)	0.2739 (5)
C(9)	0.2479 (4)	0.0658 (7)	0.4173 (4)
C(10)	0.2413 (5)	0.0941 (8)	0.3252 (6)
C(11)	0.1698 (5)	0.3059 (7)	−0.2323 (4)
C(12)	0.1667 (6)	0.5088 (8)	−0.1668 (5)
C(13)	0.0465 (7)	0.3510 (14)	−0.1495 (6)
C(14)	0.0274 (6)	0.2557 (10)	−0.0962 (6)
C(15)	0.0702 (6)	0.2979 (9)	0.0597 (5)
C(16)	0.1230 (7)	0.1008 (12)	0.0066 (8)
C(17)	0.2205 (12)	0.0596 (10)	0.0235 (11)
C(18)	0.3123 (6)	0.0482 (7)	−0.0824 (5)
C(19)	0.3948 (9)	0.1139 (8)	0.0629 (5)
N(1)	0.1499 (4)	0.3729 (6)	−0.1566 (3)
N(2)	0.1017 (4)	0.2367 (6)	0.0111 (4)
N(3)	0.2948 (4)	0.1164 (4)	−0.0083 (3)
Li(1)	0.2402 (6)	0.3118 (8)	−0.0277 (5)
Li(2)	−0.0782 (7)	0.0368 (9)	0.5109 (6)

scheme (*k* = 0.03) gave a value of $R_2 = [\Sigma w(|F_o| - |F_c|)^2 / \Sigma w|F_o|]^2 = 0.137$ at convergence.

Anisotropic thermal parameters were then used for all nonhydrogen atoms and primary and secondary anomalous dispersion corrections were applied to the iron atom scattering factor. Further least-squares refinement, using observed reflections only, gave at final convergence $R_2 = 0.061$ and $\text{ERF} = [\Sigma w(|F_o| - |F_c|)^2 / (\text{NO} - \text{NV})]^{1/2} = 2.24$, where NO is the number of reflections used in refinement and NV is the number of parameters varied. A final difference Fourier showed four peaks between 0.30 and 0.35 e/Å³; three were near the iron atom while the fourth was near C(17). A test of the weighting scheme showed no significant variation of $w(F_o - F_c)^2$ with the magnitude of the *F*_{obsd} or increasing sin θ/λ . The scattering factors for C⁰, N⁰, Li⁰, and Fe⁰ were taken from the compilation of Hanson et al.⁸ and those for hydrogen are the best spherical form factors of Stewart et al.⁹ The anomalous dispersion correction factors for iron were those of Cromer and Liberman.¹⁰

The final positional and thermal parameters for the nonhydrogen atoms are contained in Tables I and II, respectively. Table III gives the hydrogen atom positions and thermal parameters. Bond distances and angles are given in Tables IV and V, respectively. Structure factors are listed in Table VI (microfilm edition).

Discussion

Molecular Geometry and Amine-Coordinated Lithium Atom.

There are a number of unusual features associated with the structure of this molecule. These are (1) the presence of two distinct lithium atoms and the fact that even though the complex was obtained in the presence of excess base only one lithium atom is coordinated to the triamine ligand, (2) a four-center electron-deficient bridge, and (3) the relatively short lithium–iron atom–atom distance. The overall molecular geometry is shown in Figure 1. As shown in this figure, in the solid state dilithioferrocene pentamethyldiethylenetriamine exists as a dimer which is formed by two lithium atoms bridging between a single carbon atom from each of the two cyclopentadienyl rings. A crystallographic inversion center in the middle of the four-atom group which forms the bridge relates the monomeric units. The compound contains both unsolvated lithium atoms (Li(2) and Li(2')) forming the bridge and solvated lithium atoms (Li(1) and Li(1')) forming the bridge and coordinated to three PMDT nitrogen atoms. Only two other

Table II. Anisotropic Thermal Parameters for the Nonhydrogen Atoms in Dilithioferrocene PMDT

atom	β_{11}^a	β_{22}	β_{33}	β_{12}	β_{13}	β_{23}
Fe	0.006 40 (5)	0.011 85 (9)	0.004 86 (4)	0.000 53 (7)	0.002 16 (3)	0.002 17 (6)
C(1)	0.0066 (4)	0.0134 (8)	0.0060 (3)	0.0022 (5)	0.0025 (3)	0.0021 (4)
C(2)	0.0065 (4)	0.0191 (9)	0.0075 (4)	-0.0007 (6)	0.0015 (3)	0.0002 (6)
C(3)	0.0080 (5)	0.0280 (13)	0.0065 (4)	0.0033 (7)	0.0027 (4)	0.0069 (6)
C(4)	0.0118 (7)	0.0134 (9)	0.0115 (6)	0.0028 (6)	0.0057 (4)	0.0058 (6)
C(5)	0.0130 (6)	0.0135 (8)	0.0079 (4)	0.0011 (6)	0.0045 (4)	-0.0001 (5)
C(6)	0.0069 (4)	0.0150 (8)	0.0062 (3)	0.0032 (5)	0.0030 (3)	0.0033 (4)
C(7)	0.0141 (6)	0.0154 (8)	0.0063 (4)	0.0043 (6)	0.0050 (4)	0.0025 (5)
C(8)	0.0138 (8)	0.0275 (14)	0.0081 (5)	0.0079 (8)	0.0071 (5)	0.0068 (7)
C(9)	0.0065 (4)	0.0243 (11)	0.0086 (4)	-0.0001 (6)	0.0010 (3)	0.0066 (6)
C(10)	0.0065 (5)	0.0265 (14)	0.0116 (6)	0.0004 (7)	0.0037 (4)	0.0101 (8)
C(11)	0.0157 (8)	0.0214 (11)	0.0069 (4)	-0.0012 (7)	0.0014 (4)	0.0001 (6)
C(12)	0.0171 (8)	0.0201 (12)	0.0088 (5)	0.0068 (8)	0.0026 (5)	0.0027 (6)
C(13)	0.0098 (7)	0.0665 (31)	0.0096 (6)	0.0018 (12)	0.0002 (5)	0.0119 (11)
C(14)	0.0083 (6)	0.0400 (19)	0.0113 (6)	-0.0031 (6)	0.0020 (5)	0.0055 (9)
C(15)	0.0127 (7)	0.0404 (18)	0.0117 (6)	-0.0063 (9)	0.0080 (5)	-0.0010 (9)
C(16)	0.0120 (7)	0.0301 (20)	0.0163 (8)	-0.0098 (11)	0.0012 (6)	0.0089 (10)
C(17)	0.0334 (20)	0.0180 (14)	0.0391 (19)	0.0050 (14)	0.0268 (18)	0.0124 (13)
C(18)	0.0174 (8)	0.0211 (11)	0.0082 (4)	0.0044 (7)	0.0031 (5)	-0.0023 (6)
C(19)	0.0279 (13)	0.0215 (14)	0.0091 (5)	0.0085 (10)	-0.0010 (7)	-0.0003 (7)
N(1)	0.0078 (4)	0.0206 (8)	0.0053 (3)	0.0000 (5)	0.0014 (3)	0.0021 (4)
N(2)	0.0070 (4)	0.0240 (10)	0.0065 (3)	-0.0025 (5)	0.0017 (3)	0.0029 (5)
N(3)	0.0124 (5)	0.0121 (7)	0.0073 (3)	0.0007 (4)	0.0044 (3)	0.0005 (4)
Li(1)	0.0053 (6)	0.0114 (11)	0.0047 (4)	-0.0009 (6)	0.0012 (4)	0.0000 (6)
Li(2)	0.0078 (7)	0.0145 (12)	0.0059 (5)	0.0027 (7)	0.0036 (5)	0.0029 (6)

^a The form of the anisotropic ellipsoid is $\exp[-(\beta_{11}h^2 + \beta_{22}k^2 + \beta_{33}l^2 + 2\beta_{12}hk + 2\beta_{13}hl + 2\beta_{23}kl)]$.

Table III. Positional Parameters and Isotropic Thermal Parameters for the Hydrogen Atoms in Dilithioferrocene PMDT

atom	<i>x</i>	<i>y</i>	<i>z</i>	<i>B</i> ^a
H(2)	-0.0946	-0.0113	0.2908	6.27
H(3)	-0.0420	0.1511	0.1879	6.67
H(4)	0.0632	0.3284	0.2875	6.93
H(5)	0.0659	0.2775	0.4488	7.06
H(7)	0.1212	-0.1755	0.3124	6.73
H(8)	0.1672	-0.0122	0.2068	7.70
H(9)	0.2835	0.1215	0.4690	7.02
H(10)	0.2707	0.1710	0.3027	6.92
H(111)	0.2416	0.3242	-0.2342	8.24
H(112)	0.1609	0.2119	-0.2257	8.24
H(113)	0.1203	0.3366	-0.2894	8.24
H(121)	0.2385	0.5225	-0.1710	9.37
H(122)	0.1167	0.5411	-0.2228	9.37
H(123)	0.1574	0.5565	-0.1138	9.37
H(131)	0.0030	0.3306	-0.2125	12.90
H(132)	0.0224	0.4329	-0.1297	12.90
H(141)	-0.0395	0.2785	-0.0833	10.36
H(142)	0.0195	0.1745	-0.1301	10.36
H(151)	0.1234	0.2824	0.1182	10.43
H(152)	0.0627	0.3917	0.1479	10.43
H(153)	0.0031	0.2610	0.0625	10.43
H(161)	0.0823	0.0522	-0.0472	11.28
H(162)	0.0992	0.0772	0.0599	11.28
H(171)	0.2481	0.0600	0.0905	15.46
H(172)	0.2154	-0.0309	0.0013	15.46
H(181)	0.3668	0.0926	-0.1033	8.87
H(182)	0.3350	-0.0411	-0.0633	8.87
H(183)	0.2472	0.0451	-0.1325	8.87
H(191)	0.4492	0.1555	0.0398	11.64
H(192)	0.3883	0.1621	0.1169	11.64
H(193)	0.4151	0.0235	0.0801	11.64

^a The form of the isotropic thermal parameter is $\exp[-\beta(\sin^2 \theta / \lambda^2)]$.

organolithium structures have shown lithium atoms in two distinctly different environments.^{11b,12}

The coordination sphere around Li(1) consists of the cyclopentadienyl carbon atom C(6) and the three tertiary amine nitrogen atoms from one PMDT molecule. The geometry around Li(1) is roughly tetrahedral. The Li(1)-N(1) and

Li(1)-N(2) bond lengths of 2.130 (9) and 2.115 (9) Å, respectively, differ by less than two standard deviations, and are only slightly shorter (~0.04 Å) than the Li(1)-N(3) distance of 2.162 (9) Å. A similar range of lithium-nitrogen atom distances was observed in stilbene bis(lithium pentamethyldiethylenetriamine),¹⁴ although all lithium-nitrogen atom dis-

Table IV. Interatomic Distances (Å) for the Nonhydrogen Atoms in Dilithioferrocene PMDT

atoms	distance	atoms	distance
Fe-C(1)	2.119 (5) ^a	Li(1)-C(6)	2.112 (10)
Fe-C(2)	2.017 (5)	Li(1)-N(1)	2.130 (9)
Fe-C(3)	2.014 (6)	Li(1)-N(2)	2.115 (9)
Fe-C(4)	2.012 (6)	Li(1)-N(3)	2.162 (10)
Fe-C(5)	2.022 (6)	Li(2)-C(1)	2.146 (10)
Fe-C(6)	2.109 (5)	Li(2)-C(1)	2.193 (10)
Fe-C(7)	2.042 (6)	Li(2)-C(6)	2.123 (10)
Fe-C(8)	2.015 (7)	Li(2)-Li(2')	2.367 (17)
Fe-C(9)	2.024 (6)	Li(2)-Fe	2.667 (8)
Fe-C(10)	2.021 (6)	N(1)-C(11)	1.455 (8)
C(1)-C(2)	1.431 (7)	N(1)-C(12)	1.452 (9)
C(2)-C(3)	1.412 (8)	N(1)-C(13)	1.455 (10)
C(3)-C(4)	1.375 (9)	N(2)-C(14)	1.433 (9)
C(4)-C(5)	1.403 (8)	N(2)-C(15)	1.435 (9)
C(1)-C(5)	1.417 (7)	N(2)-C(16)	1.458 (11)
C(6)-C(7)	1.464 (7)	N(3)-C(17)	1.373 (11)
C(6)-C(9)	1.431 (8)	N(3)-C(18)	1.427 (7)
C(7)-C(8)	1.409 (8)	N(3)-C(19)	1.491 (9)
C(8)-C(10)	1.389 (9)	C(13)-C(14)	1.363 (12)
C(9)-C(10)	1.437 (9)	C(16)-C(17)	1.344 (13)

^a Errors in the lattice parameters are included in the estimated standard deviations.

Table V. Bond Angles (deg) for the Nonhydrogen Atoms in Dilithioferrocene PMDT

atoms	angles	atoms	angles
C(5)-C(1)-C(2)	100.3 (5) ^a	C(12)-N(1)-C(13)	110.2 (7)
C(1)-C(2)-C(3)	112.1 (6)	C(12)-N(1)-C(11)	108.2 (5)
C(2)-C(3)-C(4)	107.6 (6)	C(11)-N(1)-C(13)	112.7 (6)
C(3)-C(4)-C(5)	105.9 (6)	Li(1)-N(1)-C(11)	115.2 (5)
C(1)-C(5)-C(4)	114.1 (6)	Li(1)-N(1)-C(12)	109.1 (5)
C(7)-C(6)-C(9)	101.9 (5)	Li(1)-N(1)-C(13)	101.2 (5)
C(6)-C(7)-C(8)	111.1 (6)	C(14)-N(2)-C(15)	111.1 (6)
C(7)-C(8)-C(10)	108.4 (6)	C(14)-N(2)-C(16)	111.0 (7)
C(8)-C(10)-C(9)	106.8 (6)	C(15)-N(2)-C(16)	112.0 (7)
C(6)-C(9)-C(10)	111.8 (6)	Li(1)-N(2)-C(14)	104.8 (5)
N(1)-Li(1)-N(2)	85.9 (3)	Li(1)-N(2)-C(15)	113.1 (5)
N(2)-Li(1)-N(3)	85.1 (4)	Li(1)-N(2)-C(16)	104.3 (5)
N(1)-Li(1)-N(3)	119.8 (4)	C(17)-N(3)-C(18)	112.2 (8)
C(6)-Li(1)-N(1)	120.3 (5)	C(17)-N(3)-C(19)	109.4 (9)
C(6)-Li(1)-N(2)	109.8 (4)	C(18)-N(3)-C(19)	105.4 (6)
C(6)-Li(1)-N(3)	118.7 (4)	Li(1)-N(3)-C(17)	101.6 (6)
C(1)-Li(2)-C(1')	113.9 (4)	Li(1)-N(3)-C(18)	119.1 (5)
C(1')-Li(2)-C(6)	144.9 (5)	Li(1)-N(3)-C(19)	108.9 (5)
C(1)-Li(2)-C(6)	101.2 (4)	N(1)-C(13)-C(14)	120.8 (8)
Li(2)-C(1)-C(6)	66.1 (4)	C(13)-C(14)-N(2)	117.1 (7)
C(1)-Li(2)-Fe	50.6 (2)	N(2)-C(16)-C(17)	118.7 (8)
C(6)-Li(2)-Fe	50.7 (2)	C(16)-C(17)-N(3)	124.8 (10)

^a Errors in the lattice parameters are included in the estimated standard deviations.

tances are shorter in dilithioferrocene-PMDT than in stilbene bis(lithium pentamethyldiethylenetriamine). The nitrogen-lithium-nitrogen bond angles of 85.9 (3)° for N(1)-Li(1)-N(2) and 85.1 (4)° for N(2)-Li(1)-N(3) are similar to those previously found in complexes containing the lithium-TMED group.¹³

Lithium Atom (2) Geometry. Carbon atoms C(1), C(6), and C(1') are located 2.146 (10), 2.123 (10), and 2.193 (10) Å, respectively, from Li(2) and are disposed in a roughly trigonal geometry about Li(2). The Li(2)-C(6) bond length is the second shortest known lithium-carbon distance. Li(2) and Li(2') are 2.367 (17) Å apart; this is comparable to the lithium-lithium distances of 2.424 and 2.397 Å found in ethyllithium¹⁵ and cyclohexyllithium,¹⁶ respectively, and might suggest a direct lithium-lithium interaction in dilithioferrocene-PMDT. However, based on previous NMR¹⁷ and Raman¹⁸ studies, and the description of the bonding in cyclohexyllithium,¹⁶ it is felt that there is little direct lithium-lithium bonding present here. Li(2) can complete its coordi-

nation sphere by utilizing its one remaining 2p orbital which is not involved in three-center electron-deficient bonding with the nearby cyclopentadienyl carbon atoms, to overlap with the nonbonding ferrocene e_g molecular orbital. The Li(2)-Fe separation of 2.667 (8) Å is comparable to the sum (2.68 Å) of the covalent radii for each metal (1.34 Å for lithium^{19b} and 1.34 Å for iron²⁰).

Covalent metal-iron bonding has been found in two compounds^{20,21} similar to dilithioferrocene-PMDT, while transition metal-lithium bonding^{11,12,19,22-25} has been observed in several complexes and appears to be important in helping to stabilize them. An iron-magnesium bond distance of 2.593 (7) Å is found in $(\eta^5-C_5H_5)(diphos)FeMgBr \cdot 2(C_4H_8O)$,²¹ while in $(\eta^5-C_5H_5)Fe(\eta^5-C_5H_4)Au_2(PPh_3)_2]^+$ the iron-gold distance is 2.818 (9) Å.²⁰ A range of distances from 2.40 to 2.79 Å has been found in complexes containing transition metal-lithium atom bonding. In the π -dinitrogen-nickel-lithium complex $[(C_6H_5Li)_6Ni_2N_2(C_4H_{10}O)_2]_2$,¹¹ there are lithium atoms which bridge the nickel-nickel bond or are

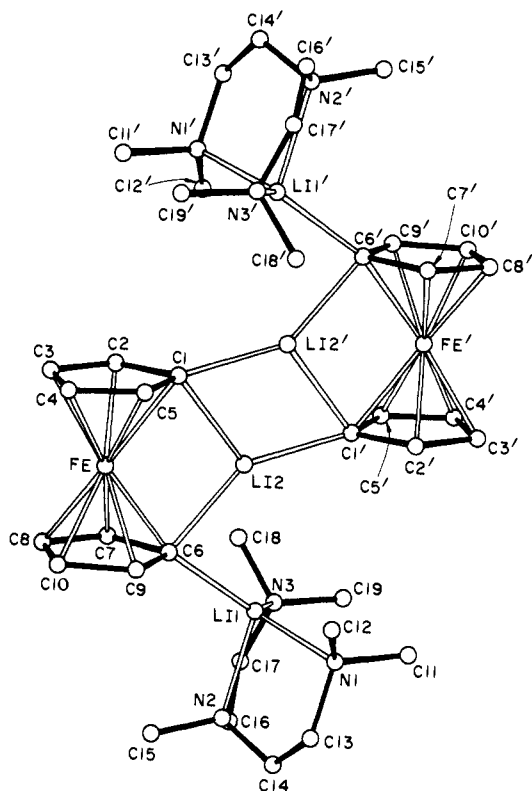


Figure 1. Molecular structure of $[(\eta^5\text{-C}_5\text{H}_4)_2\text{Fe}(\text{N}_3\text{C}_9\text{H}_{23})\text{Li}_2]_2$.

bonded to only one nickel atom. The nickel–lithium distances vary between 2.61 and 2.79 Å. The existence of π bonding of dinitrogen to nickel was attributed to the Lewis acid properties of Li^+ enhancing back-bonding from the nickel atom to the nitrogen molecule. In $[(\eta^5\text{-C}_5\text{H}_5)_2\text{M}(\text{H})\text{Li}]_4$ ($\text{M} = \text{Mo}$ or W),¹⁹ transition metal to lithium bonding gives rise to the formation of the eight-membered ring of alternating lithium and group 6 atoms. The average M–Li bond lengths found were 2.70 Å for molybdenum and 2.69 Å for tungsten. In each of the compounds $\text{Li}_4\text{Cr}_2(\text{CH}_3)_8\cdot 4\text{C}_4\text{H}_8\text{O}$ (I),²³ $\text{Li}_4\text{Cr}_2(\text{C}_4\text{H}_8)_4\cdot 4\text{C}_4\text{H}_{10}\text{O}$ (II),²⁴ and $\text{Li}_4\text{Mo}_2(\text{CH}_3)_8\cdot 4\text{C}_4\text{H}_8\text{O}$ (III),²⁵ the carbon atoms of the M_2C_8 core ($\text{M} = \text{Cr}$ or Mo) form a parallelepiped, with one lithium atom over the center of each vertical face. For each compound, it has been proposed that the four lithium atoms interact with the π and δ electrons in the M–M quadrupole bond, and in the chromium complexes, this interaction stabilizes these compounds. The M–Li distances are 2.558 (28) Å in I, 2.54 (5) to 2.71 (6) Å in II, and approximately 2.7 Å in III. The lithium to midpoint of the M–M bond distances are 2.388 (28) Å in I, 2.398 (51) and 2.486 (60) Å in II, and approximately 2.5 Å in III. Our results suggest that iron–lithium atom bonding is also present in $[(\eta^5\text{-C}_5\text{H}_4)_2\text{Fe}(\text{N}_3\text{C}_9\text{H}_{23})\text{Li}_2]_2$ and that this bonding contributes to the stability of the dimeric structure which is observed.

Ferrocenyl Group Geometry. The two cyclopentadienyl rings are nearly eclipsed, with C(1)–C(2)–C(3)–C(4)–C(5) (plane 1) opposite C(6)–C(7)–C(8)–C(10)–C(9) (plane 2) (Figure 2). The relative rotational orientation between the two rings, as defined by Churchill and Wormald,²⁶ is approximately 4°. Palenik²⁷ has noted that the preferred configuration of ferrocene derivatives will be eclipsed, or nearly so. Here, however, bonding constraints involving Li(2) probably require an eclipsed or nearly eclipsed configuration. Within experimental error each ring is planar and the two rings are nearly parallel; the angle between planes is 2.0 (5)°. This angle is similar to that found in several other structures of substituted ferrocenes.^{26–29} C(4) and C(10) show the smallest distance of

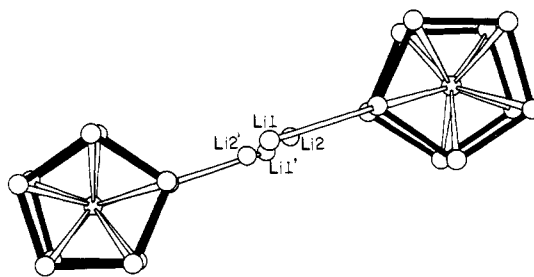


Figure 2. View of $\text{Li}_4\text{Fe}_2(\text{C}_5\text{H}_4)_4$ fragment of the structure showing the nearly coplanar configuration of the six metal atoms and the eclipsed configuration of the cyclopentadienyl rings. The PMDT fragments have been omitted for clarity.

separation, while C(1) and C(6) show the greatest. These data, although at a marginal level of significance, suggest that the presence of Li(2) between C(1) and C(6) has caused the rings to tilt slightly. This is also reflected in the interatomic distances.

The average for all five iron–ring carbon atom distances to each ring is 2.037 (9) Å for plane 1 and 2.042 (9) Å for plane 2, which compares favorably with the range of 2.03–2.06 Å previously observed.²⁶ However, the Fe–C(1) distance of 2.119 (5) Å and Fe–C(6) distance of 2.109 (5) Å are considerably longer than the remaining four iron–ring carbon distances and when the Fe–C(1) and Fe–C(6) distances are excluded, the average iron–ring carbon atom distances become 2.016 (9) Å for plane 1 and 2.026 (9) Å for plane 2.

The carbon–carbon bond lengths average 1.408 (12) Å in plane 1 and 1.426 (12) Å in plane 2. These values are within the range of distances previously reported.^{26–29} The longest and shortest distances in each ring are directly opposite each other; the C(1)–C(2) and C(6)–C(7) distances of 1.431 (7) and 1.464 (7) Å, respectively, are the longest, while the C(3)–C(4) and C(8) and C(10) distances of 1.375 (9) and 1.389 (8) Å, respectively, are the shortest.

PMDT Molecule. There appears to be some disorder present in the PMDT molecule. The root mean square displacements of the nitrogen atoms indicate that these atoms are not disordered. Rather, the problem is the same as that previously observed in triphenylmethyl lithium *N,N,N,N*-tetramethylethylenediamine³³ and bifluorenyl bis(lithium *N,N,N,N*-tetramethylethylenediamine).³⁴ The distances for the two methylene carbon–methylene carbon bonds—1.363 (12) Å for C(13)–C(14) and 1.344 (13) Å for C(16)–C(17)—are shorter than expected. The nature of the disorder is probably the same in all three compounds. The nitrogen atom positions are fixed, but there are two possible configurations for the methylene atoms which rapidly interconvert. While the anisotropic thermal parameters alone probably adequately compensate for the motion of the PMDT methyl carbon atoms, both the anisotropic thermal parameters and positional parameters of the methylene carbon atoms have refined to best fit the observed electron density distribution, resulting in apparently short carbon–carbon bond lengths.

NMR Spectroscopy. The ferrocenyllithium complex exhibits stereochemical nonrigidity. The observed ¹H NMR spectra for the cyclopentadienyl rings and the PMDT base are shown in Figures 3, 4, and 5, respectively. The low-temperature limiting spectra can be explained on the basis of the solid-state structure. As shown in Figure 1, two nonequivalent cyclopentadienyl rings exist; a Li–PMDT moiety is bonded to one cyclopentadienyl ring while two unsolvated lithium atoms are bonded to the other. In solution a plane of symmetry is postulated containing all four lithium atoms and bisecting each PMDT and ferrocene moiety. This plane of symmetry is shown in Figure 2. Thus four nonequivalent cyclopentadienyl protons of equal intensity would be expected and are observed (Figure

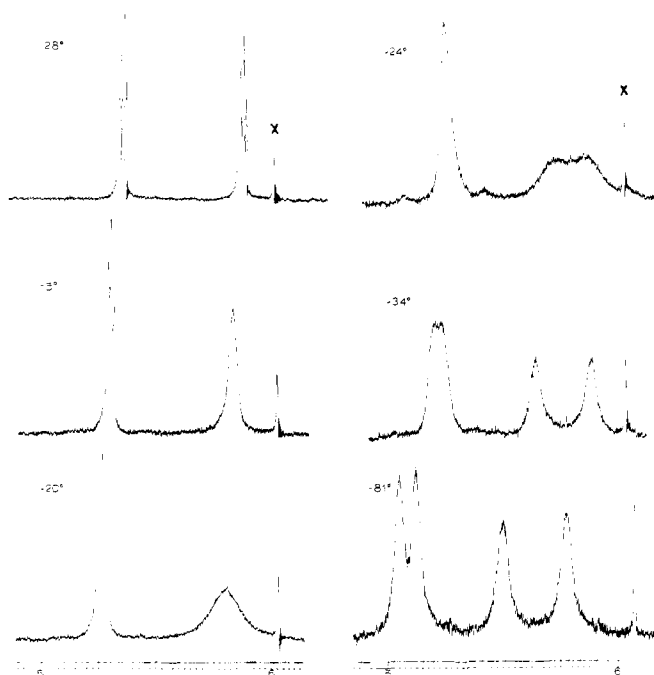


Figure 3. Temperature-dependent ^1H NMR spectra of cyclopentadienyl rings in $[(\eta^5\text{-C}_5\text{H}_4)_2\text{Fe}(\text{N}_3\text{C}_9\text{H}_{23})\text{Li}_2]_2$. The peak denoted by an X is a ferrocene impurity. Scale is in units of τ .

3) corresponding to the protons (using the numbering in Figure 1) H_2H_5 , H_7H_9 , H_3H_4 , and H_8H_{10} . The peak at τ 6.03 (denoted by an X) that remains a sharp singlet throughout the temperature range investigated is a ferrocene impurity. At -81°C the peaks at τ 5.51 and 5.78 are assigned to the protons closest to the lithium atoms while the peaks at τ 5.06 and 5.13 are assigned to the cyclopentadienyl protons furthest from the lithium atoms, since it is assumed that they (protons H_3H_4 and H_8H_{10}) would be in a similar chemical environment and hence have similar chemical shifts.

Raising the temperature causes the cyclopentadienyl peaks to coalesce until finally the high-temperature limiting spectrum at 28°C consists of two triplets ($J = 1.25$ Hz) corresponding to the four protons closest to the lithium atoms and the four protons furthest away. These are actually AA'XX' patterns with $|J_{\text{AX}} + J_{\text{AX}'}| = 1.25$ Hz. Taking the spectral coalescence points to be 241 and 251 K with a chemical shift difference of 6.5 and 27.5 Hz, respectively, we estimate ΔG^\ddagger at coalescence to be 12.7 ± 1.0 and 12.6 ± 1.0 kcal/mol, respectively,³⁵ indicating that a single exchange process is equilibrating the cyclopentadienyl rings.

The spectra for the PMDT is much more complicated. In accordance with the solid-state structure, the low-temperature limiting spectra (Figure 4) shows five proton resonances (the sharp quintet marked Y is an impurity in toluene- d_8) corresponding to the three nonequivalent methyl groups and the two nonequivalent methylene protons. Increasing the temperature causes dramatic changes in the spectra until three proton resonances are observed for the high-temperature limiting spectra obtained at 75°C (Figure 5). Based on the integration of the NMR spectrum, these resonances can be assigned to the methyl groups on the terminal nitrogen atoms, the methylene protons, and the methyl group on the middle nitrogen atom of the PMDT base, respectively. Although there are two distinct types of methylene protons, only a single peak is observed. This is probably due to the similarity of their chemical environments, causing an overlap of two peaks. Throughout the region $28\text{--}75^\circ\text{C}$, the cyclopentadienyl triplets remain unchanged. This seems to suggest two exchange processes occurring, one involving the PMDT and cyclopentadienyl rings and the second

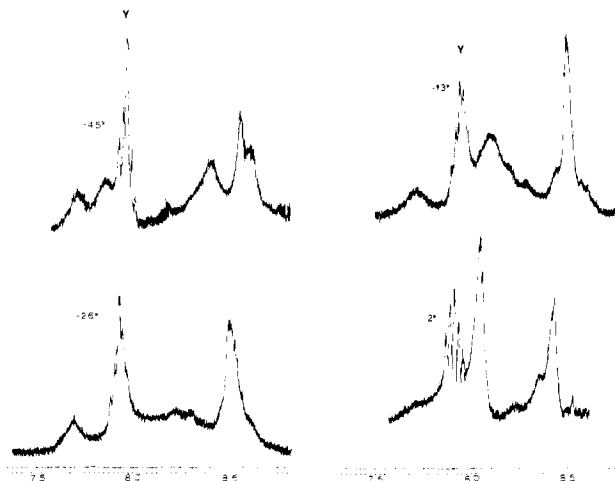


Figure 4. Low-temperature ^1H NMR spectra of PMDT ligand in $[(\eta^5\text{-C}_5\text{H}_4)_2\text{Fe}(\text{N}_3\text{C}_9\text{H}_{23})\text{Li}_2]_2$. The quintet indicated by a Y is an impurity in toluene- d_8 . The scale is in units of τ .

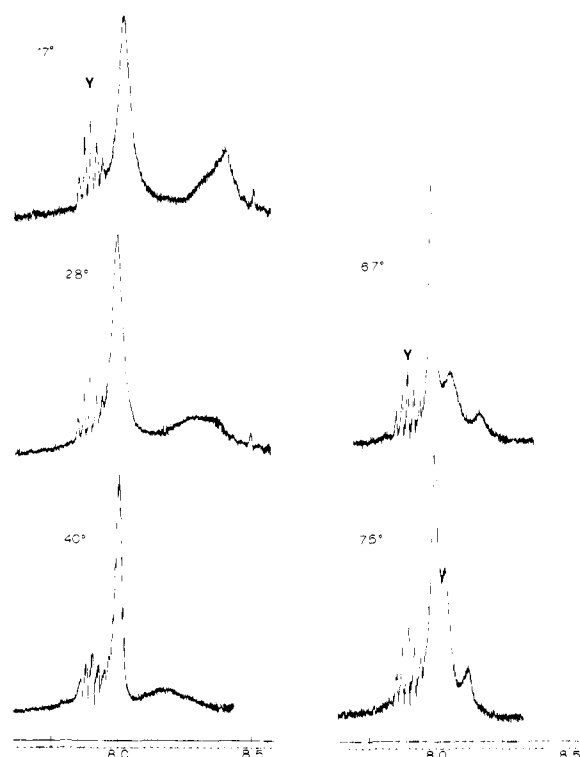
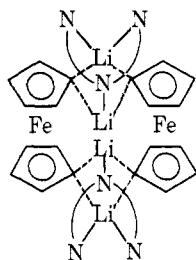


Figure 5. High-temperature ^1H NMR spectra of PMDT ligand in $[(\eta^5\text{-C}_5\text{H}_4)_2\text{Fe}(\text{N}_3\text{C}_9\text{H}_{23})\text{Li}_2]_2$. The quintet indicated by a Y is an impurity in toluene- d_8 . The scale is in units of τ .

involving the PMDT only. In a separate experiment, it is found that free PMDT exchanges with the coordinated PMDT in the ferrocenyllithium complex over a similar temperature range.

The establishment of an exact mechanism is not possible owing to the complexity of the PMDT NMR spectra. However, an attractive possibility involves the dissociation of the PMDT nitrogen atoms from the solvated lithium atom onto the unsolvated lithium atom with the simultaneous breaking of a $\text{Li}(2)\text{-C}$ bond. This, followed by a rotation of a ferrocene group, leads to a plane of symmetry that bisects the ferrocene moiety, thus equilibrating the two cyclopentadienyl rings. A possible transition state is shown below. At higher temperatures the PMDT completely dissociates where it is free to rotate and undergo rapid inversion.



We have attempted to investigate the ^7Li NMR spectrum but could not obtain any signal at room temperature, although one resonance was observed at higher temperatures. The absence of a signal at room temperature could be due to quadrupolar relaxation of the nitrogen atoms on the PMDT molecule.

Acknowledgment. The financial support of the National Science Foundation under DMR-77 2-3999 and CHE 77 24964 is gratefully acknowledged. A NSF departmental equipment grant to the University of Illinois made the NMR studies possible and is also appreciated.

Supplementary Material Available: Structure factor tables (Table 6) for $[(\eta^5\text{-C}_5\text{H}_4)_2\text{Fe}(\text{N}_3\text{C}_9\text{H}_{23})\text{Li}_2]_2$ (4 pages). Ordering information is given on any current masthead page.

References and Notes

- (1) (a) University of Illinois; (b) University of Massachusetts.
- (2) (a) For a review of some early work, see D. W. Slocum, T. R. Engelmann, C. Ernst, C. A. Jennings, W. Jones, B. Koonvitsky, J. Lewis, and P. Shenkin, *J. Chem. Educ.*, **46**, 144 (1969). (b) D. E. Bublitz and K. L. Rinehart, Jr., *Org. React.*, **17**, 1 (1969).
- (3) R. F. Kovar, M. D. Rausch, and H. Rosenberg, *Organomet. Chem. Synth.*, **1**, 173 (1970-1971).
- (4) M. D. Rausch and D. J. Ciappenelli, *J. Organomet. Chem.*, **10**, 127 (1967).

- (5) J. J. Bishop, A. Davison, M. L. Katcher, D. W. Lichtenberger, R. E. Merrill, and J. C. Smart, *J. Organomet. Chem.*, **27**, 241 (1971).
- (6) M. D. Rausch, G. A. Moser, and C. F. Meade, *J. Organomet. Chem.*, **51**, 1 (1973).
- (7) J. J. Brooks, W. Rhine, and G. D. Stucky, *J. Am. Chem. Soc.*, **94**, 7339 (1972).
- (8) H. P. Hanson, F. Herman, J. D. Lea, and S. Skillman, *Acta Crystallogr.*, **17**, 1040 (1964).
- (9) R. F. Stewart, E. R. Davidson, and W. T. Simpson, *J. Chem. Phys.*, **42**, 3175 (1965).
- (10) D. T. Cromer and D. Liberman, *J. Chem. Phys.*, **53**, 1891 (1970).
- (11) (a) K. Jonas, *Angew. Chem., Int. Ed. Engl.*, **12**, 997 (1973); (b) C. Krüger and Y.-H. Tsay, *ibid.*, **12**, 998 (1973).
- (12) D. J. Brauer, C. Krüger, and Y.-H. Tsay, Abstracts, Eighth International Conference of Organometallic Chemistry, p 123.
- (13) G. D. Stucky, *Adv. Chem. Ser.*, **130**, 56 (1974).
- (14) M. R. Walczak and G. D. Stucky, *J. Am. Chem. Soc.*, **98**, 5531 (1976).
- (15) H. Dietrich, *Acta Crystallogr.*, **16**, 681 (1963).
- (16) R. Zenger, W. Rhine, and G. D. Stucky, *J. Am. Chem. Soc.*, **96**, 6048 (1974).
- (17) T. L. Brown, L. M. Seitz, and B. Y. Kimura, *J. Am. Chem. Soc.*, **90**, 3245 (1968).
- (18) W. M. Scovell, B. Y. Kimura, and T. G. Spiro, *J. Coord. Chem.*, **1**, 107 (1971).
- (19) (a) F. W. S. Benfield, R. A. Forder, M. L. H. Green, G. A. Moser, and C. K. Prout, *J. Chem. Soc., Chem. Commun.*, 759 (1973); (b) R. A. Forder and C. K. Prout, *Acta Crystallogr., Sect. B*, **30**, 3218 (1974).
- (20) V. G. Andrianov, Yu. T. Struchkov, and E. R. Rossinskaja, *J. Chem. Soc., Chem. Commun.*, 338 (1973).
- (21) H. Felkin, P. J. Knowles, B. Meunier, A. Mitschler, L. Ricard, and R. Weiss, *J. Chem. Soc., Chem. Commun.*, 44 (1974).
- (22) Reference 5 cited in ref 12.
- (23) J. Krausse, G. Marx, and G. Schödl, *J. Organomet. Chem.*, **21**, 159 (1970).
- (24) J. Krausse and G. Schödl, *J. Organomet. Chem.*, **27**, 59 (1971).
- (25) F. A. Cotton, J. M. Troup, T. R. Webb, D. H. Williamson, and G. Wilkinson, *J. Am. Chem. Soc.*, **96**, 3824 (1974).
- (26) M. R. Churchill and J. Wormald, *Inorg. Chem.*, **8**, 716 (1969).
- (27) G. J. Palenik, *Inorg. Chem.*, **9**, 2424 (1969).
- (28) A. P. Krukoniis, J. Silverman, and N. F. Yannoni, *Acta Crystallogr., Sect. B*, **28**, 987 (1972).
- (29) L. H. Brown and G. M. Brown, *Acta Crystallogr., Sect. B*, **27**, 81 (1971).
- (30) L. F. Battelle, R. Bau, G. W. Gokel, R. T. Dyakawa, and I. K. Ugi, *J. Am. Chem. Soc.*, **95**, 482 (1973).
- (31) M. R. Churchill and K. L. Kalra, *Inorg. Chem.*, **12**, 1650 (1973).
- (32) J. Trotter, *Acta Crystallogr.*, **11**, 355 (1958).
- (33) J. J. Brooks and G. D. Stucky, *J. Am. Chem. Soc.*, **94**, 7333 (1972).
- (34) M. R. Walczak and G. D. Stucky, *J. Organomet. Chem.*, **97**, 313 (1977).
- (35) H. Kessler, *Angew. Chem., Int. Ed. Engl.*, **9**, 219 (1970).

Nucleophilic Substitution at Phosphorus. The Effect of Ion Association on the Stereochemistry and Rate of Substitution at Phosphorus in a Six-Membered Ring Phosphate¹

Mike Bauman and William S. Wadsworth, Jr.*

Contribution from the Department of Chemistry, South Dakota State University, Brookings, South Dakota 57007. Received November 17, 1977

Abstract: The *cis*- and less stable *trans*-2-*p*-nitrophenyl-5-chloromethyl-5-methyl-2-oxo-1,3,2-dioxaphosphorinans undergo substitution with an oxy anion to give both inversion and retention products. The product isomer ratio is highly dependent upon the degree of anion-cation association which in turn is dependent upon the nature of the cation and solvent. A high degree of ion association favors the retention pathway. The results are interpreted by assuming a square pyramidal intermediate with the anion-cation complex spanning the phosphoryl oxygen bond.

Nucleophilic substitution at tetravalent phosphorus, e.g., phosphate triesters, is presently discussed in terms of trigonal bipyramidal (TBP) transition states or intermediates.² Hydrolysis studies with ^{18}O have ruled out an addition-elimination mechanism.^{3a-c} A TBP intermediate has been invoked, however, to explain, by means of suitable pseudorotational permutations, retention at phosphorus,^{4a-d} a route which often accompanies the assumed normal inversion path.⁵

Difficulties arise in devising mechanisms which adhere to

the principle of microscopic reversibility and meet the requirement that ligands prefer to enter and leave from apical positions. The choice between retention and inversion is assumed to rest with the relative apicophilicity of the ligands in the intermediate TBP phosphorane.⁶ However, recent variable temperature NMR studies^{7a-c} indicate similar apicophilicities for groups which normally are displaced by different pathways.

Owing to its conformationally rigid ring, the 2-substituted